Regular Article – Atomic and Molecular Collisions

Fragmentation dynamics of diatomic molecules under proton impact: Kinetic energy release spectra of CO^{q+} and NO^{q+} (q = 2, 3) molecular ions

Avijit Duley[1], Narendra Nath Dutta[2], C. Bagdia[3], L. C. Tribedi[3], C. P. Safvan[4], and A.H. Kelkar[1,a]

[1] Indian Institute of Technology Kanpur, Kanpur 208016, India
[2] School of Sciences, SR University, Warangal, India
[3] Tata Institute of Fundamental Research, 1 Homi Bhabha Road Colaba, Mumbai 400005, India
[4] Inter-University Accelerator Centre, Aruna Asif Ali Marg, New Delhi 110067, India

Abstract. We report the fragmentation dynamics of triply charged, diatomic, molecular ions of NO and CO. Dissociative fragmentation after multiple ionization of NO and CO is studied under the impact of 200 keV proton beam using a recoil-ion momentum spectrometer. Kinetic Energy Release distributions (KERDs) for various fragmentation channels were obtained. We have also calculated the potential energy curves (PECs) for ground and several excited states of NO^{3+} and CO^{3+} molecular ions using the multi-reference configuration interaction (MRCI) method. The obtained KERDs are discussed in the background of the calculated PECs as well as the simple Coulomb excitation model. Coulomb breakup of the unstable precursor molecular ion shows a clear preference for the $N^{2+} + O^+$ (and $C^{2+} + O^+$) fragmentation channel.

1 Introduction

The study of ionization and fragmentation dynamics of small and large molecules is an active area of atomic physics research. Fragmentation of molecular ions leads to the creation of atomic ions and free radicals. The creation and evolution of such ionic and neutral fragments is a key aspect in understanding the processes related to plasma physics, atmospheric and space physics, radiation damage, etc. In a laboratory environment, the precursor molecular ion can be generated by collisions of neutral molecules with photons, electrons or heavy ion projectile beams. The advent of recoil ion momentum spectrometer (RIMS) [1], along with a position-sensitive detector, allows for detailed investigation of the subsequent molecular fragmentation process. In the past couple of decades, there have been extensive studies on the dissociation dynamics of multiply charged molecular ions produced in collisions with heavy ions [1–4], electrons [5–8] and photons [9,10]. Although the target molecules under investigation range from diatomic molecules to polyatomic systems, including large bio-molecules and PAHs (polycyclic aromatic hydrocarbons), it is the diatomics which have been studied extensively.

Several studies (experimental and theoretical) have investigated the ionization and fragmentation of simple diatomics such as N_2, O_2 and CO under particle and photon impact. In collisions where the ionization and subsequent Coulomb fragmentation of the precursor molecular ion take place at time scales shorter than the vibrational time period of the molecular ion, the kinetic energy release distribution (KERD) provides complete information of the internal excitation of the molecular ion. The KER values observed experimentally can be directly compared with calculated potential energy curves (PECs) for the neutral and ionized molecule. The electronic states and corresponding PECs for neutral, singly ionized, and doubly ionized diatoms are readily available in the literature [11–15]. However, such calculations for multiply charged molecular ions are rather limited [16–18]. For example, there are very few reports on the fragmentation dynamics of NO molecule [19–22] and the PEC calculations are available only up to doubly charged (NO^{2+}) molecular ions [15,19,23].

In order to produce multiply charged molecular ions, sufficient energy needs to be deposited in the neutral molecule to cause multi-electron ionization/excitation. Collisions with energetic heavy ion beams are the most efficient way of producing multiple ionization in the parent molecule. Additionally, in collisions with heavy-ion beams with hundreds of keV energy, the interaction time is less than a few femtoseconds. This interaction time is shorter than the typical vibrational and rotational time scales of the molecules, and hence, the electronic excitation of the molecule is a Franck–Condon transition. Therefore, the KER depends on the internu-

clear separation, which is characteristic of the precursor molecular ion state.

In this paper, we present our combined experimental and theoretical study on the fragmentation of triply charged NO^{3+} and CO^{3+} molecular ions produced in collisions of the neutral molecules with 200 keV proton beam. Kinetic energy release distributions have been obtained for NO^{q+} and CO^{q+} ($q = 2,3$) molecular ions. We have also calculated the energy of excited electronic states and corresponding PECs for triply charged molecular ions. The theoretical PECs for CO^{3+} compare well with existing calculations, whereas for NO^{3+} molecular ion the PECs have not been reported previously.

2 Experiment and data analysis

The experiments were performed at two accelerator facilities in India. Measurements with CO molecular target were performed at 300 keV ECR ion accelerator (ECRIA) at TIFR, Mumbai. For the NO molecular target, the experiments were performed at the low energy ion beam facility (LEIBF) at IUAC, New Delhi. The time-of-flight mass spectrometer (TOFMS) setup at both the accelerator facilities are very similar and have been described in detail elsewhere [25, 26]. Briefly, a collimated beam of 200 keV (250 keV for NO) protons was made to collide with an effusive molecular gas target in a high vacuum scattering chamber. The recoil ions, following a collision, were extracted by a TOFMS located perpendicular to the projectile ion beam as well as the gas jet. A channel electron multiplier (CEM) was used to detect the electrons emitted in the ionization process. The output signal from the CEM was used as a start signal for the data acquisition system. The dissociated ionic fragments were detected on the other end of the TOFMS using a micro-channel plate (MCP) detector equipped with a position-sensitive delay line anode (DLD). Signals from the MCP and the DLD were fed to a multi-hit time to digital converter (TDC). The TDC allows the detection of both ionic fragments from a single dissociation event. Analysis of the coincidence data was performed on an event-by-event basis to obtain the 3D momenta of the ionic fragments. The three momenta of each ion pair were then used to obtain the KERD for a given dissociation channel.

In the present projectile energy range, charge exchange processes such as electron capture may also contribute to multiple ionization of the diatomic molecules. However, in the present experiments, we have not analyzed the projectile beam after the collisions. Hence, the data presented are integrated over all processes leading to multiple ionization and fragmentation of the parent molecule.

3 Theoretical potential energy curves

In order to calculate the potential energy curves (PECs) for the CO^{3+} and NO^{3+} molecular ions, we have first obtained the PECs for the ground states of CO and NO molecules. The ground states of CO and NO molecules are $^1\Sigma^+$ and $^2\Pi$, respectively. The PECs are calculated using the multi-reference configuration interaction (MRCI) method with complete active space self-consistent field (CASSCF) reference functions. For CASSCF calculations, we have considered the full-valence type active space. We have used the MOL-PRO software package [27] which uses an internally contracted version of the MRCI approach (icMRCI) [28–30] for robust and accurate generations of the PECs at various internuclear separations (grid points). The basis set used in our calculations is the correlation consistent cc-pV5Z basis set.

We have calculated these PECs for a sufficiently large set of grid points starting from 0.8 Å to 4.0 Å to ensure the position of the minima for both CO and NO molecules. The minimum for the $^1\Sigma^+(^2\Pi)$ state of neutral CO(NO) molecule occurs at an inter-nuclear separation of 1.13 Å (1.15 Å) with a dissociation energy of 11.17 eV (6.46 eV). The corresponding experimental values reported previously are 1.128 Å (1.154 Å) [31] and 11.09 eV (6.496 eV) [32] for CO(NO) molecule. The PECs for the $CO^{3+}(NO^{3+})$ molecular ions are calculated with respect to the total molecular energies obtained at the minimum of the $^1\Sigma^+$ ($^2\Pi$) state. Similar to the neutral counterparts, we adopt the icMRCI approach based on CASSCF reference functions with full-valence active space and cc-pV5Z basis sets to calculate the PECs for these ionic systems. However, unlike neutral CO and NO, our aim is to calculate 3 states for each of the 8 symmetries: $^2\Sigma^+$, $^4\Sigma^+$, $^2\Sigma^-$, $^4\Sigma^-$, $^2\Pi$, $^4\Pi$, $^2\Delta$, $^4\Delta$ for CO^{3+}, and $^1\Sigma^+$, $^1\Sigma^-$, $^3\Sigma^+$, $^3\Sigma^-$, $^1\Pi$, $^3\Pi$, $^1\Delta$, $^3\Delta$ for NO^{3+}. Hence, to have balanced descriptions of the orbitals for all the three states of a particular symmetry, we have chosen a state-average CASSCF approach for each symmetry. The grid points for the PECs of these ionized species are calculated from 0.9 to 2.00 Å with grid separation of 0.05 Å and then from 2.00 to 3.00 Å with grid separation of 0.10 Å. However, the grid points are adjusted (by a minimal amount) in very few cases where proper convergence is not achieved during icMRCI calculations. In general, calculations of the PECs up to 3 Å are sufficient to identify the channels of atomic fragmentation for the 24 states calculated for each of the triply ionized molecules. From around 2.5 Å, the PECs are almost consistent with the fall with increasing internuclear separation as expected following the equation $E_{AB}(\mathrm{eV}) = E_A(\mathrm{eV}) + E_B(\mathrm{eV}) + 14.4\frac{q_A q_B}{R}$ [6]. Here, E_{AB} is the total energy of the molecular state, $E_A(E_B)$ and $q_A(q_B)$ are the energy, and charge of the fragment ions at the dissociation limit of the state, and R is the internuclear separation in Å. The last term of this equation represents the Coulomb repulsion energy (in eV)

between two charged particles kept at a distance of R apart.

The vertical excitation energies for the first states of $^4\Sigma^-$, $^2\Sigma^+$, $^2\Pi$ and $^2\Delta$ symmetries of CO^{3+} are calculated to be 81.92 eV, 83.17 eV, 81.32 eV, and 83.83 eV, respectively. These results agree quite well with similar calculations with cc-pVQZ basis sets performed by Kumar and Sathyamurthy [33]. They obtained these values 81.82 eV, 82.63 eV, 81.26 eV, and 83.13 eV, respectively. Also, our estimated value of 83.83 eV for the first state of $^2\Delta$ symmetry is in good agreement with the experimental value of 83.4 eV [34,35]. The energy states of the fragmented ions, C^+, C^{2+}, N^+, N^{2+}, O^+ and O^{2+} are calculated using the same icM-RCI approach and the same quality of basis functions. The excitation energies between the different states are compared with the corresponding values obtained from the atomic spectra database of the National Institute of Standards and Technology (NIST) [36], and good agreements were found between these two sets of energies.

4 Results and discussions

In ion-molecule collision experiments, the molecular ion can be created in multiple charge states depending on the degree of parent ionization. The multiply ionized parent molecular ion is short-lived due to mutual Coulomb repulsion between the two (for diatomic molecules) nuclear centers and dissociates into fragment ions. In previous studies with highly charged heavy ions with CO, multiply charged molecular ions up to CO^{7+} have been observed [37]. On the other hand, a few hundred keV protons act as relatively soft projectiles resulting in mainly doubly and triply ionized molecular ions. In the present measurements, we have observed parent molecular ions up to CO^{4+} and NO^{4+}. However, the discussion is limited to the dissociation of doubly and triply charged molecular ions as the yield for quadruply charged ion was rather small. We have measured the kinetic energy release distributions for a) the single symmetric dissociation channel of CO^{2+} and NO^{2+} molecular ions and b) the two asymmetric dissociation channels of CO^{3+} and NO^{3+} molecular ions. In Table 1, we have listed the experimentally observed most probable KER values for each dissociation channel. The KER values calculated using the simple Coulomb explosion model are also shown in the same table.

The Coulomb explosion model is a simple model describing the fragmentation of molecular ions. In this model, the individual atomic centers of the parent molecular ion are considered as point charges, and the Coulomb repulsion between these atoms determines the kinetic energy release of the dissociation process. The energy expected from this model is given by: $E(\text{eV}) = 14.4 \frac{q_A q_B}{R_e(\text{Å})}$, where q_A and q_B are the asymptotic charges of the two fragments, and R_e is the equilibrium internal nuclear distance of the neutral molecule. R_e corre-

sponds to the distance from which vertical transition is expected to take place according to the Franck–Condon principle. However, the model excludes the effect of the charge cloud in the inter-nuclear region as well as the electron correlation effects. Therefore, the Coulomb explosion model is known to predict KER values higher than those obtained experimentally [38].

Thus, it is intuitive to assume that the most probable KER value is smaller than that predicted by the Coulomb explosion model. However, in the present experiment, we have found an opposite trend in the case of NO^{3+} molecular ion. The most probable KER value for the dissociation of NO^{3+} lies above the Coulomb energy. A multi-charged diatomic molecule can accommodate a large number of repulsive potential energy curves, giving rise to a wide range of KERs. If low-lying molecular states are characterized by high electron densities in the internuclear region, it will generally give KER values less than the Coulomb energy. Whereas highly excited molecular states with significantly reduced nuclear screening can give KER values greater than the Coulomb energy [39].

4.1 Dissociation of CO^{2+} and NO^{2+}

The experimentally observed KER spectra for dissociation of doubly charged CO^{2+} and NO^{2+} molecular ions are shown in Figs. 1 and 2. The doubly charged parent molecular ion dissociates into singly charged fragments, $C^+ + O^+$ (and $N^+ + O^+$) due to mutual repulsion, which is the most dominant fragmentation channel for this collision system. Dissociation into a charged and a neutral fragment cannot be observed with our present experimental setups. The KER spectrum for CO^{2+} fragmentation channel after collision with photons [40,41] and charged particles [6,7,34,37,39] has been reported by several groups. The most probable KER value measured in this experiment (see Table 1) and the overall
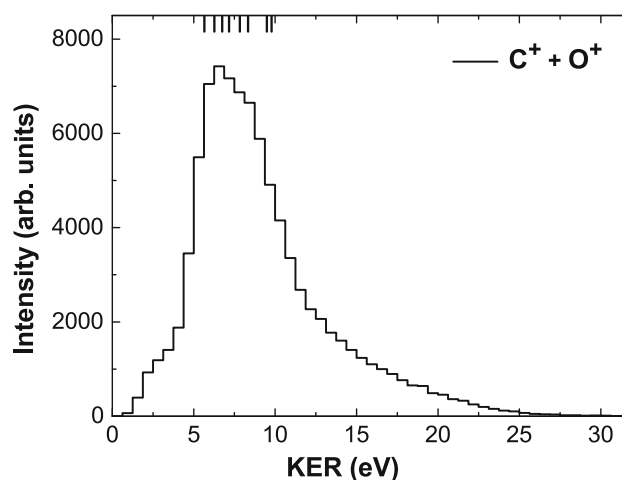

Fig. 1 Kinetic energy release spectra for the fragmentation of CO^{2+} molecular ion. Theoretical values [24] are indicated by vertical lines at the top of the graph
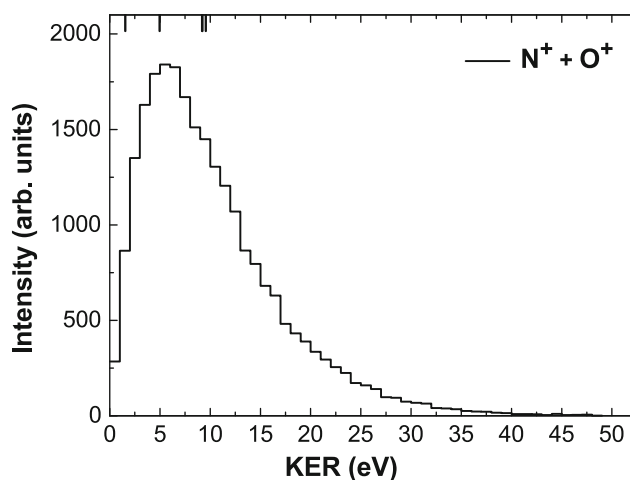
Fig. 2 Kinetic energy release spectra for the fragmentation of NO^{2+} molecular ion. Theoretical values [14,19,23] are indicated by vertical lines at the top of the graph
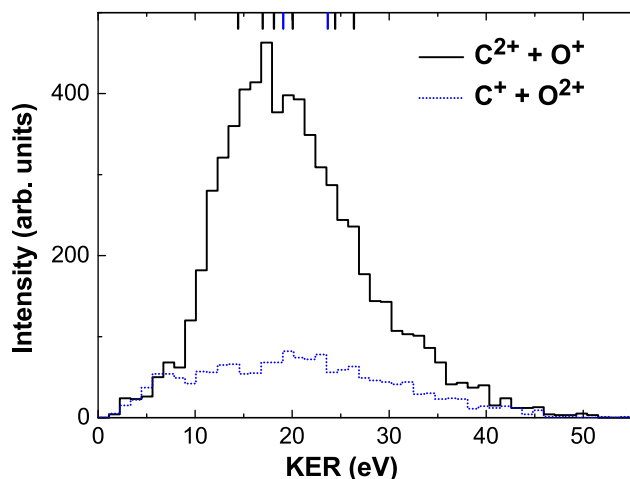

Fig. 3 (Color online) Kinetic energy release spectra for CO^{3+} fragmentation. Theoretical values obtained from CASSCF-MRCI calculations are indicated by vertical lines at the top of the graph for both channel 1 (black) and channel 2 (blue)

Fig. 4 Kinetic energy release spectra for NO^{3+} fragmentation. Theoretical values obtained from CASSCF-MRCI calculations are indicated by vertical lines at the top of the graph for both channel 1 (black) and channel 2 (blue)

shape of the KER distribution are in agreement with the reported values in the literature [34,37,39,42–44].

The observed KER values can be accounted for by considering three low-lying electronic states of CO^{2+} ion [24]. The KER spectra contains contributions from $1^1\Sigma^+, 1^1\Pi$ and $X^3\Pi$ dissociating into ground state products of $C^+(^2P) + O^+(^4S)$. It is to be noted that the KERD has a long tail up to 30 eV, which may arise due to the participation of higher electronic states of the precursor ion. Dissociation dynamics of the NO molecule has not been studied as extensively as the CO molecular target. Nevertheless, few experimental studies have been reported for NO^{2+} fragmentation in collisions with photons [9,45,46] and electrons [5,47]. The KER spectrum is similar to that obtained for CO^{2+} ion. The potential energy curves (PECs) for NO^{2+} have
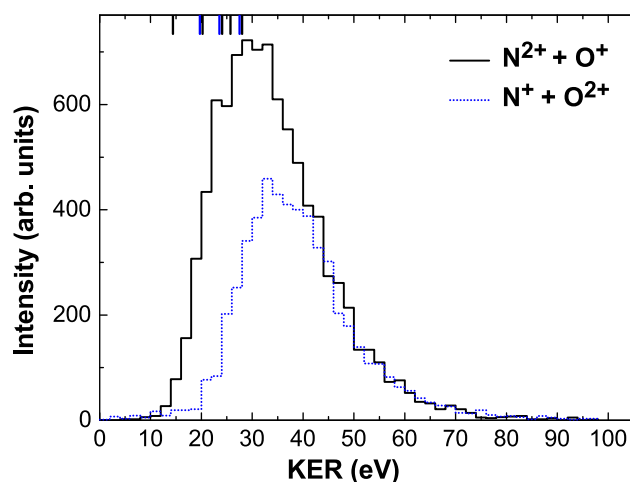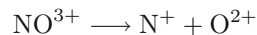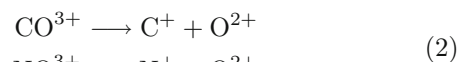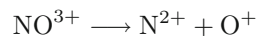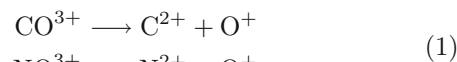
been calculated by various groups [14,19,23]. One can associate the measured KER spectra with a few prominent PECs. For both CO^{2+} and NO^{2+} fragmentation, it is seen that the most probable KER value is much smaller than that calculated using the Coulomb explosion model. However, the tail of KER spectra extends well beyond this value on the high-energy side. Such large KER can be attributed to the high lying electronic states of the doubly charged parent molecular ion. The high lying electronic states are more repulsive due to a steeper slope in the Franck–Condon region owing to the weaker screening of the positive nuclear centers, thus leading to a higher KER of the fragment ions.

4.2 Dissociation of CO^{3+} and NO^{3+}

The dissociation of a triply charged heteroatomic molecular ion such as CO^{3+} or NO^{3+} can proceed via two channels where the total electronic charge of the parent molecular ion is shared asymmetrically by the two fragment ions. The two possible fragmentation channels are represented as channel 1 and channel 2 as below:

$$
\begin{aligned}
CO^{3+} &\longrightarrow C^{2+} + O^+ \\
NO^{3+} &\longrightarrow N^{2+} + O^+
\end{aligned}
\tag{1}
$$

$$
\begin{aligned}
CO^{3+} &\longrightarrow C^+ + O^{2+} \\
NO^{3+} &\longrightarrow N^+ + O^{2+}
\end{aligned}
\tag{2}
$$

The KER spectra for these two fragmentation channels are shown in Figs. 3 and 4. It is observed that channel 1 is the dominant mode for charge asymmetric dissociation. In Table 1, we have shown the relative intensities of channels 1 and 2. In the case of CO^{3+} dissociation, the measured yield of channel 1 is ~ 4 times

larger than channel 2. The same in the case of NO³⁺ dissociation is found to be ∼ 2. The dominance of channel 1 over channel 2 has also been seen in previous studies with CO molecular target [42,48–50]. The reported ratio varies from 2 to 5 depending on the charge, mass, and energy of the projectile ion. Similar data for NO³⁺ dissociation, however, have not been reported so far. The dissociation dynamics of CO^{3+} molecular ion has been discussed in detail by Handke et al. [18]. The authors performed a three-hole population analysis, characterizing the distribution of positive charge on the two nuclear centers, for the creation of CO^{3+} molecular ion. It was shown that after the Franck–Condon transition all states of the triply charged molecular ion were characterized by charge delocalization, with slight preference for channel 2 over channel 1. This is contrary to the experimental observations. On the other hand, the calculated PECs (in [18] as well as in the present work) clearly show a number of curve crossings, even for low lying states, resulting in strong interaction between different molecular states. Therefore, the dissociation of the parent molecular ion may not proceed along one particular PEC following vertical transition. According to Handke *et al.*, the charge distribution switches during the dissociation process resulting in predominance of channels 1 over 2.

The difference in the yield of the two dissociation channels can be explained based on the ionization potential of the two participating atoms. The ionization potential of the Carbon (and Nitrogen) atom is smaller compared to that of the Oxygen atom. Subsequently, the total energy needed to create the final dissociation state is 49.3 eV and 64.2 eV (CO³⁺ and NO³⁺, respectively) for channel 1 as opposed to 59.9 eV and 69.7 eV for channel 2 [34,51]. A relatively larger yield of channel 2 in the case of NO³⁺ dissociation is in agreement with the smaller difference in ionization energies of the final state fragment ions.

The most probable values of KERD differ slightly for channel 1 and channel 2, as listed in Table 1. The KER spectrum for CO³⁺ fragmentation can be compared with previous experimental investigations. The most probable KER value depends on the choice of the projectile, and values ranging from 11 eV to 27 eV have been reported for channel 1 [8,37,43]. For channel 2, the

most probable KER value is generally higher than that for channel 1. The difference in most probable KER appears to be strongly dependent on the choice of the projectile. For example, with heavy-ion projectiles in the MeV range, the most probable KER for dissociation via channel 2 has been shown to be ∼ 10 eV larger than that for channel 1. In collisions with photons, this difference is much smaller [52]. In the present experiments with 200 keV proton, this difference is also not very large (see table 1). The evolution of the most probable KER values can be investigated in relation to the interaction strength of the projectile. Collisions with photons and electrons fall under perturbative regime where multiple ionization of the molecular ion is accompanied by excitation to low-lying dissociating states. This results in lower value of most probable KER when compared with the Coulomb explosion model. Whereas, collisions with heavy ion projectile lead to predominant excitation to high-lying dissociating states of the multi charged molecular ion. This results in a broader KER distribution and a larger value of most probable KER, comparable to that predicted by the Coulomb explosion model. In addition, studies on molecular fragmentation with highly charged ions (HCIs) have shown that the high Coulomb field of the outgoing projectile also affects the KER distribution [53].

The KER spectra can be compared with the calculated potential energy curves for CO³⁺ and NO³⁺ molecular ions. As stated earlier, numerous theoretical calculations are available for CO³⁺. However, the theoretical potential energy curves for excited states of NO³⁺ molecular ions have not been reported. In Tables 2 and 3, we have listed the calculated PECs for CO³⁺ and NO³⁺ molecular ions, respectively. The observed KER spectra are in good agreement with the calculated PEC values. In Figs. 5 and 6, we have also shown the PECs for a few selected states. The steep slope and repulsive nature of excited states give rise to higher KER. We also observe that for the case of NO³⁺ fragmentation, the higher excited states appear to contribute dominantly, resulting in a larger value of the most probable KER.

The KER values discussed above are based on the direct dissociation of the molecular ion, where it evolves only on a single PEC. A molecular ion can also disso-

Table 1 Experimentally Observed most probable values in the KER spectra for the various fragmentation channels for CO^{q+} and NO^{q+} ($q = 2, 3$) fragmentation induced by proton impact. The values calculated from a pure Coulomb explosion model are also included

Fragmentation channel	KER (eV)	Coulomb energies (eV)	Relative intensity (%)
C⁺ + O⁺	6 ± 0.6	12.8^a	91.51
C²⁺ + O⁺	16 ± 1	25.5^a	6.76
C⁺ + O²⁺	19 ± 1	25.5^a	1.73
N⁺ + O⁺	5 ± 1	12.52^b	62.87
N²⁺ + O⁺	29 ± 2	25.04^b	23.34
N⁺ + O²⁺	32 ± 2	25.04^b	13.8

^{a}At equilibrium distance of 1.128 Å
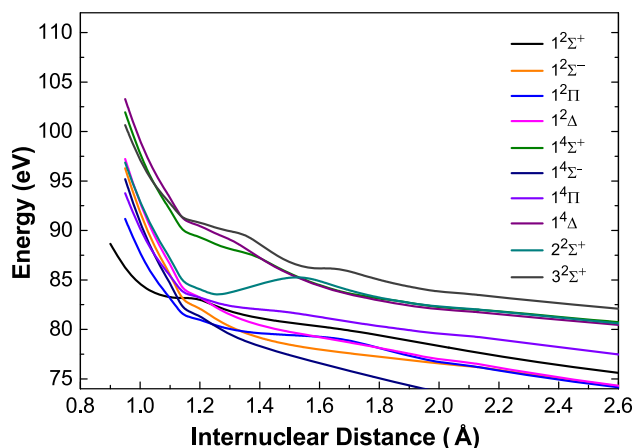^{b}At equilibrium distance of 1.151Å

Fig. 5 (Color online) Potential Energy Curves from CASSCF-MRCI calculations on CO^{3+}. The zero point on the vertical scale corresponds to the minimum of the $^1\Sigma^+$ ground state of neutral CO molecule
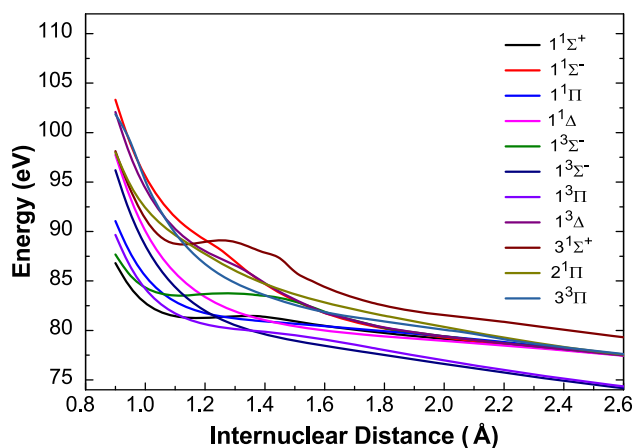

Fig. 6 (Color online) Potential Energy Curves from CASSCF-MRCI calculations on NO^{3+}. The zero point on the vertical scale corresponds to the minimum of the $^2\Pi$ ground state of neutral NO molecule

Table 2 The possible molecular states of CO^{3+} dissociating into $C^{2+} + O^+$ and $C^+ + O^{2+}$ along with the KER values obtained from the PEC calculation. The KER values are also compared with that from Ref. [34]

Molecular states	Dissociation limit	KER (eV) (calc.)	KER (eV) [34]
$1^2\Sigma^+$	$C^{2+}(^1S) + O^+(^2P)$	16.97	–
$2^2\Sigma^+$	$C^{2+}(^3P) + O^+(^2D)$	14.42	13.74
$3^2\Sigma^+$	$C^{2+}(^3P) + O^+(^2P)$	19.93	–
$1^2\Sigma^-$	$C^{2+}(^1S) + O^+(^2D)$	19.53	19.55
$2^2\Sigma^-$	$C^{2+}(^3P) + O^+(^4S)$	26.37	–
$3^2\Sigma^-$	$C^{2+}(^3P) + O^+(^2D)$	24.42	–
$1^2\Pi$	$C^{2+}(^1S) + O^+(^2D)$	18.13	–
$2^2\Pi$	$C^{2+}(^1S) + O^+(^2P)$	19.83	–
$3^2\Pi$	$C^{2+}(^3P) + O^+(^4S)$	20.49	–
$1^2\Delta$	$C^{2+}(^1S) + O^+(^2D)$	20.64	21.25
$2^2\Delta$	$C^{2+}(^3P) + O^+(^2D)$	22.89	–
$3^2\Delta$	$C^{2+}(^3P) + O^+(^2D)$	23.44	–
$1^4\Sigma^+$	$C^{2+}(^3P) + O^+(^2D)$	20.06	–
$2^4\Sigma^+$	$C^{2+}(^3P) + O^+(^2P)$	22.85	–
$3^4\Sigma^+$	$C^{2+}(^3P) + O^+(^2P)$	29.01	–
$1^4\Sigma^-$	$C^{2+}(^1S) + O^+(^4S)$	22.07	22.72
$2^4\Sigma^-$	$C^{2+}(^3P) + O^+(^4S)$	23.52	–
$3^4\Sigma^-$	$C^{2+}(^3P) + O^+(^2D)$	22.94	–
$1^4\Pi$	$C^{2+}(^3P) + O^+(^4S)$	17.21	17.85
$2^4\Pi$	$C^{2+}(^3P) + O^+(^2D)$	19.30	–
$3^4\Pi$	$C^{2+}(^3P) + O^+(^2D)$	24.29	–
$1^4\Delta$	$C^{2+}(^3P) + O^+(^2D)$	21.21	–
$2^4\Delta$	$C^{2+}(^3P) + O^+(^2D)$	24.37	–
$3^2\Sigma^+$	$C^+(^2P) + O^{2+}(^3P)$	19.07	–
$2^4\Sigma^+$	$C^+(^2P) + O^{2+}(^3P)$	23.66	–

ciate via indirect processes. Predissociation is one such indirect process, where a molecular ion jumps from one PEC to another during dissociation due to coupling with another PEC. Now, two PECs can couple with each other through spin-orbit interaction. And, according to the rules of the spin-orbit interaction [54], the coupling can only happen between molecular states of different symmetries. The rate of predissociation would depend on the Franck–Condon (FC) factor between the two participating PECs as well as on the position of the crossing point [55]. Although we have not calculated the different vibrational states of PECs, their lifetime, or FC factors, our calculation clearly shows the crossing of repulsive states with molecular states having local minima.

Among all the calculated PECs of CO^{3+}, only one molecular state can predissociate via spin-orbit coupling, which is the $2^2\Sigma^+$ state. It has a local minimum

at 1.2 Å, with a potential barrier height of 1.75 eV. And, it has a dissociation limit of $C^{2+}(^3P) + O^+(^2D)$ with KER of 14.42 eV. This state is crossed by the $2^2\Pi$ repulsive state at an internuclear separations of around 1.13 Å (obtained by B-Spline fit to the calculated values). Thus, $2^2\Sigma^+$ state can predissociate via the $2^2\Pi$ into $C^{2+}(^1S) + O^+(^2P)$ producing a KER of 19.26 eV. On the other hand, for NO^{3+}, there are two possible candidates for predissociation. The calculated PEC for $1^1\Sigma^+$ state of NO^{3+} has a local minimum at 1.15 Å, with a potential barrier height of 218 meV. And, it has a dissociation limit of $N^{2+}(^2P) + O^+(^2D)$ with KER of 14.42 eV. This state is crossed by the $1^3\Pi$ repulsive state at an internuclear separation of around 1.13 Å (obtained by B-Spline fit to the calculated values). Thus, $1^1\Sigma^+$ state can predissociate via the $1^3\Pi$ into $N^{2+}(^2P) + O^+(^4S)$ producing a KER of 17.76 eV. Similarly, $3^1\Sigma^+$ state of NO^{3+} has a local minimum at 1.15Å with a potential barrier height of 372 meV. And, it has a dissociation limit of $N^{2+}(^2P) + O^+(^2P)$ with KER of 20.22 eV. The two repulsive states $2^1\Pi$ and $3^3\Pi$ cross the $3^1\Sigma^+$ state at an internuclear separation of around 1.15 Å (obtained by B-Spline fit to the calculated values). Thus, $1^1\Sigma^+$ state can predissociate via the $2^1\Pi$ or $3^3\Pi$ into $N^{2+}(^2P) + O^+(^2D)$ producing

Table 3 The possible molecular states of NO^{3+} dissociating into $N^{2+}+O^+$ and $O^{2+}+N^+$ along with the theoretically calculated values of KER

Molecular states	Dissociation limit	KER (eV) (calc.)
$1^1\Sigma^+$	$N^{2+}(^2P) + O^+(^2D)$	14.42
$2^1\Sigma^+$	$N^{2+}(^2P) + O^+(^2P)$	16.45
$3^1\Sigma^+$	$N^{2+}(^2P) + O^+(^2P)$	20.22
$1^1\Sigma^-$	$N^{2+}(^2P) + O^+(^2D)$	23.32
$2^1\Sigma^-$	$N^{2+}(^2P) + O^+(^2D)$	25.72
$3^1\Sigma^-$	$N^{2+}(^2P) + O^+(^2P)$	28.02
$1^1\Pi$	$N^{2+}(^2P) + O^+(^2D)$	15.37
$2^1\Pi$	$N^{2+}(^2P) + O^+(^2D)$	21.81
$3^1\Pi$	$N^{2+}(^2P) + O^+(^2D)$	24.70
$1^1\Delta$	$N^{2+}(^2P) + O^+(^2D)$	17.58
$2^1\Delta$	$N^{2+}(^2P) + O^+(^2D)$	24.02
$3^1\Delta$	$N^{2+}(^2P) + O^+(^2P)$	27.99
$1^3\Sigma^+$	$N^{2+}(^2P) + O^+(^2D)$	16.72
$2^3\Sigma^+$	$N^{2+}(^2P) + O^+(^2P)$	19.71
$3^3\Sigma^+$	$N^{2+}(^2P) + O^+(^2P)$	24.07
$1^3\Sigma^-$	$N^{2+}(^2P) + O^+(^4S)$	19.52
$2^3\Sigma^-$	$N^{2+}(^2P) + O^+(^2D)$	23.30
$3^3\Sigma^-$	$N^{2+}(^2P) + O^+(^2D)$	26.13
$1^3\Pi$	$N^{2+}(^2P) + O^+(^4S)$	17.56
$2^3\Pi$	$N^{2+}(^2P) + O^+(^2D)$	18.94
$3^3\Pi$	$N^{2+}(^2P) + O^+(^2D)$	21.23
$1^3\Delta$	$N^{2+}(^2P) + O^+(^2D)$	22.13
$2^3\Delta$	$N^{2+}(^2P) + O^+(^2D)$	25.76
$3^3\Delta$	$N^{2+}(^2P) + O^+(^2P)$	24.49
$3^1\Sigma^+$	$N^+(^3P) + O^{2+}(^3P)$	19.69
$3^1\Sigma^-$	$N^+(^3P) + O^{2+}(^3P)$	27.49
$3^1\Delta$	$N^+(^3P) + O^{2+}(^3P)$	27.47
$3^3\Sigma^+$	$N^+(^3P) + O^{2+}(^3P)$	23.55
$3^3\Delta$	$N^+(^3P) + O^{2+}(^3P)$	23.97

a KER of 21.89 eV. Thus, predissociation can lead to higher KER compared to the direct dissociation process. Our PEC calculation clearly explains the KER range of 14 eV to 28 eV through contributions from both pre- and direct dissociation. As discussed earlier, the high energy tail in KER distribution could be due to contributions from high lying states. Those high lying states could dissociate via direct or indirect (predissociation) process. Detailed calculations of high lying states are thus needed to explain the high energy tail of the KER spectra.

5 Conclusion

In this work, we have investigated the dissociation dynamics of multiply charged molecular ions of CO and NO. The parent molecular ions are created in ionizing collisions with 200 keV (250 keV for NO) proton. The dissociation pathways and corresponding KER spectra were measured using a recoil ion momentum spectrometer. For the fragmentation of triply charged molecular ions, a preference for the channel (channel 1) in which the carbon (nitrogen) ion carries a higher (q=2) charge is clearly observed. In addition, it is also observed that the most probable KER value is higher for the channel (channel 2) having a higher charge (q=2) on the oxygen ion. For the fragmentation of CO^{3+}, both the channels showed a most probable KER value less than the Coulomb energy. Whereas, for the case of NO^{3+} fragmentation, the most probable KER value is found to be larger than the one calculated from a simple Coulomb explosion model. This behavior was attributed to the electron cloud screening effect in the internuclear region. We have also calculated the potential energy curves of several low lying states for the triply charged CO^{3+} and NO^{3+} ions. The measured KER distribution is found to match well with the calculated PECs. For the fragmentation of both the molecular ions, we see a high energy tail, which can be attributed to the excitation of the molecular ions to high lying states. But, the calculated low lying states of the NO^{3+} molecular ion do not show a significant contribution between the most probable value and the high energy tail of the KER spectra. A few predissociating states, for both the molecular ions, have been shown to give higher KER values than the direct dissociation process. For the NO^{3+} molecular ion, there could exist high lying repulsive states which can predissociate via coupling with metastable ones. The direct and indirect dissociations from these states could contribute to the KER spectra beyond the most probable value as well as in the high-energy tail region. Detailed *ab initio* calculations of high lying states for both heteroatomic molecules are thus needed to explain the high energy region in KER spectra.

Author contributions

AHK conceived the study. AHK, AD, CB, LCT and CPS performed the experiment. NND performed theoretical calculations. AD and AHK analyzed the data. AD, NND and AHK wrote the manuscript.

References

1. J. Ullrich, R. Moshammer, R. Dörner, O. Jagutzki, V. Mergel, H. Schmidt-Böcking, L. Spielberger, Recoil-ion momentum spectroscopy. J. Phys. B Atomic Mol. Opt. Phys. **30**(13), 2917–2974 (1997)

2. J. Ullrich, R. Moshammer, A. Dorn, R. Dörner, L.P.H. Schmidt, H. Schmidt-Böcking, Recoil-ion and electron momentum spectroscopy: reaction-microscopes. Rep. Prog. Phys. **66**(9), 1463–1545 (2003)

3. I. Ben-Itzhak, K.D. Carnes, S.G. Ginther, D.T. Johnson, P.J. Norris, O.L. Weaver, Fragmentation of CH_4 caused by fast-proton impact. Phys. Rev. A **47**, 3748–3757 (1993). https://doi.org/10.1103/PhysRevA.47.3748

4. D.L. Hansen, M.E. Arrasate, J. Cotter, G.R. Fisher, K.T. Leung, J.C. Levin, R. Martin, P. Neill, R.C.C. Perera, I.A. Sellin, M. Simon, Y. Uehara, B. Vanderford, S.B. Whitfield, D.W. Lindle, Neutral dissociation of hydrogen following photoexcitation of HCl at the chlorine K edge. Phys. Rev. A **57**, 2608–2611 (1998). https://doi.org/10.1103/PhysRevA.57.2608

5. E. Fainelli, F. Maracci, R. Platania, L. Avaldi, Auger electron-ion coincidence experiment on nitric oxide molecule excited by electron impact. J. Chem. Phys. **104**(9), 3227–3233 (1996)

6. A. Pandey, B. Bapat, K.R. Shamasundar, Charge symmetric dissociation of doubly ionized N_2 and CO molecules. J. Chem. Phys. **140**(1), 034319 (2014)

7. A. Pandey, P. Kumar, S.B. Banerjee, K.P. Subramanian, B. Bapat, Electron-impact dissociative double ionization of N_2 and CO: dependence of transition probability on impact energy. Phys. Rev. A **93**, 042712 (2016). https://doi.org/10.1103/PhysRevA.93.042712

8. R. Singh, P. Bhatt, N. Yadav, R. Shanker, Ionic fragmentation of the CO molecule by impact of 10-keV electrons: Kinetic-energy-release distributions. Phys. Rev. A **87**, 022709 (2013). https://doi.org/10.1103/PhysRevA.87.022709

9. D.M. Curtis, J.H.D. Eland, Coincidence studies of doubly charged ions formed by 30.4 nm photoionization. Int. J. Mass Spectrom. Ion Processes **63**(2), 241–264 (1985)

10. P. Bolognesi, D.B. Thompson, L. Avaldi, M.A. MacDonald, M.C.A. Lopes, D.R. Cooper, G.C. King, Vibrationally selected $O^+ - O^+$ fragmentation of O_2 below the adiabatic double-ionization potential studied via electron-electron coincidence spectroscopy. Phys. Rev. Lett. **82**, 2075–2078 (1999). https://doi.org/10.1103/PhysRevLett.82.2075

11. I. Tobias, R.J. Fallon, J.T. Vanderslice, Potential energy curves for CO. J. Chem. Phys. **33**(6), 1638–1640 (1960). https://doi.org/10.1063/1.1731475

12. S.V. O'Neil, H.F. Schaefer, Valence-excited states of carbon monoxide. J. Chem. Phys. **53**(10), 3994–4004 (1970). https://doi.org/10.1063/1.1673871

13. T. Masuoka, Kinetic-energy release in the dissociation of CO^{2+}. J. Chem. Phys. **101**(1), 322–327 (1994). https://doi.org/10.1063/1.468192

14. A.C. Hurley, V.W. Maslen, Potential curves for doubly positive diatomic ions. J. Chem. Phys. **34**(6), 1919–1925 (1961)

15. R. Caprioli, J.H. Beynon, J.W. Richardson, Decomposition of metastable diatomic doubly charged positive ions. J. Am. Chem. Soc. **93**(8), 1852–1857 (1971). https://doi.org/10.1021/ja00737a003

16. V. Krishnamurthi, K. Nagesha, V.R. Marathe, D. Mathur, Probing the quantal identity of low-lying electronic states of CO^{2+} by quantum-chemical calculations and ion-translational-energy spectrometry. Phys. Rev. A **44**, 5460–5467 (1991). https://doi.org/10.1103/PhysRevA.44.5460

17. M. Larsson, B. Olsson, P. Sigray, Theoretical study of the CO^{2+} dication. Chem. Phys. **139**(2), 457–469 (1989)

18. G. Handke, F. Tarantelli, L.S. Cederbaum, Triple ionization of carbon monoxide. Phys. Rev. Lett. **76**, 896–899 (1996). https://doi.org/10.1103/PhysRevLett.76.896

19. P.W. Thulstrup, E.W. Thulstrup, A. Andersen, Y. Öhrn, Configuration interaction calculations of some observed states of NO^-, NO, NO^+, and NO^{2+}. J. Chem. Phys. **60**(10), 3975–3980 (1974)

20. T. Endo, H. Fujise, H. Hasegawa, A. Matsuda, M. Fushitani, O.I. Tolstikhin, T. Morishita, A. Hishikawa, Angle dependence of dissociative tunneling ionization of NO in asymmetric two-color intense laser fields. Phys. Rev. A **100**, 053422 (2019). https://doi.org/10.1103/PhysRevA.100.053422

21. P. Erman, P.A. Hatherly, A. Karawajczyk, U. Köble, E. Rachlew-Källne, M. Stankiewicz, K.Y. Franzén, Fragmentation processes of the core-excited NO molecule. J. Phys. B Atomic Mol. Opt. Phys. **29**(8), 1501–1513 (1996). https://doi.org/10.1088/0953-4075/29/8/014

22. W. Lai, C. Guo, The role of molecular electron distribution in strong-field ionization and dissociation of heteronuclear molecules. J. Phys. B Atomic Mol. Opt. Phys. **49**(22), 225601 (2016). https://doi.org/10.1088/0953-4075/49/22/225601

23. D.L. Cooper, Ab initio investigation of low-lying $^2\Sigma^+$ and $^2\Pi$ states of NO^{2+}. Chem. Phys. Lett. **132**(4), 377–382 (1986)

24. M. Lundqvist, P. Baltzer, D. Edvardsson, L. Karlsson, B. Wannberg, Novel time of flight instrument for doppler free kinetic energy release spectroscopy. Phys. Rev. Lett. **75**, 1058–1061 (1995). https://doi.org/10.1103/PhysRevLett.75.1058

25. S. Biswas, L.C. Tribedi, A recoil ion momentum spectrometer for probing ionization, e-capture, and capture-ionization induced molecular fragmentation dynamics. Rev. Sci. Instrum. **92**(12), 123304 (2021). https://doi.org/10.1063/5.0068307

26. A. Kumar, J. Rajput, T. Sairam, M. Jana, L. Nair, C. Safvan, Setup for measuring angular anisotropies in slow ion-molecule collisions. Int. J. Mass Spectrom. **374**, 44–48 (2014)

27. H.J. Werner, P.J. Knowles, G. Knizia, F.R. Manby, M. Schütz, Molpro: a general-purpose quantum chemistry program package. WIREs Comput. Mol. Sci. **2**(2), 242–253 (2012). https://doi.org/10.1002/wcms.82

28. H. Werner, P.J. Knowles, An efficient internally contracted multiconfiguration-reference configuration interaction method. J. Chem. Phys. **89**(9), 5803–5814 (1988). https://doi.org/10.1063/1.455556

29. P.J. Knowles, H.-J. Werner, An efficient method for the evaluation of coupling coefficients in configuration interaction calculations. Chem. Phys. Lett. **145**(6), 514–522 (1988)

30. K.R. Shamasundar, G. Knizia, H.-J. Werner, A new internally contracted multi-reference configuration interaction method. J. Chem. Phys. **135**(5), 054101 (2011). https://doi.org/10.1063/1.3609809

31. NIST Computational Chemistry Comparison and Benchmark Database NIST Standard Reference Database Number 101 Release 22, May 2022, Editor: Russell D. Johnson III. http://cccbdb.nist.gov/. https://doi.org/10.18434/T47C7Z

32. K.P. Huber, G. Herzberg, *Molecular spectra and molecular structure IV. Constants of diatomic molecules.* (Van Nostrand Reinhold, New York, 1979)

33. P. Kumar, N.P. Sathyamurthy, Potential energy curves for neutral and multiply charged carbon monoxide. Pramana-J. Phys. **74**, 49–55 (2010). https://doi.org/10.1007/s12043-010-0006-y

34. D. Mathur, E. Krishnakumar, K. Nagesha, V.R. Marathe, V. Krishnamurthi, F.A. Rajgara, U.T. Raheja, Dissociation of highly charged CO^{q+} (q>or=2) ions via non-coulombic potential energy curves. J. Phys. B Atomic Mol. Opt. Phys. **26**(6), L141 (1993). https://doi.org/10.1088/0953-4075/26/6/005

35. W. Watson, D. Stewart, A. Gardner, M. Lynch, The photoabsorption coefficients of CO and CO_2 in the region 350 to 650Å. Planet. Space Sci. **23**(2), 384–386 (1975)

36. A. Kramida, Yu. Ralchenko, J. Reader, and and NIST ASD Team. NIST Atomic Spectra Database (ver. 5.8), [Online] (National Institute of Standards and Technology, Gaithersburg, MD, 2020). Available: https://physics.nist.gov/asd [2021, June 5]

37. J. Rajput, C.P. Safvan, Kinetic energy distributions in ion-induced CO fragmentation: signature of shallow states in multiply charged CO. Phys. Rev. A **75**, 062709 (2007). https://doi.org/10.1103/PhysRevA.75.062709

38. J. Rajput, S. De, A. Roy, C.P. Safvan, Kinetic energy distributions and signature of target excitation in N_2 fragmentation on collisions with Ar^{9+} ions. Phys. Rev. A **74**, 032701 (2006). https://doi.org/10.1103/PhysRevA.74.032701

39. R.L. Watson, G. Sampoll, V. Horvat, O. Heber, Kinetic-energy release in the dissociative capture-ionization of CO molecules by 97-MeV Ar^{14+} ions. Phys. Rev. A **53**(2), 1187–1190 (1996)

40. T. Masuoka, Kinetic energy release in the dissociation of CO^{2+}. J. Chem. Phys. **101**(1), 322 (1994). https://doi.org/10.1063/1.468192

41. X. Li, J. Yu, H. Xu, X. Yu, Y. Yang, Z. Wang, P. Ma, C. Wang, F. Guo, Y. Yang, S. Luo, D. Ding, Multiorbital and excitation effects on dissociative double ionization of CO molecules in strong circularly polarized laser fields. Phys. Rev. A **100**, 013415 (2019). https://doi.org/10.1103/PhysRevA.100.013415

42. E. Wells, V. Krishnamurthi, K.D. Carnes, N.G. Johnson, H.D. Baxter, D. Moore, K.M. Bloom, B.M. Barnes, H. Tawara, I. Ben-Itzhak, Proton-carbon monoxide collisions from 10 keV to 14 MeV. Phys. Rev. A **72**(2), 022726 (2005)

43. I. Ben-Itzhak, S.G. Ginther, V. Krishnamurthi, K.D. Carnes, Kinetic-energy release in CO dissociation caused by fast F^{4+} impact. Phys. Rev. A **51**(1), 391–399 (1995)

44. H.O. Folkerts, R. Hoekstra, R. Morgenstern, Velocity and charge state dependences of molecular dissociation induced by slow multicharged ions. Phys. Rev. Lett. **77**(16), 3339–3342 (1996)

45. J.M. Curtis, R.K. Boyd, Predissociation processes in N_2^{2+}, O_2^{2+}, and NO^{2+}, studied by ion kinetic energy spectroscopy. J. Chem. Phys. **81**(7), 2991–3001 (1984)

46. T. Masuoka, Kinetic-energy release in the dissociation of NO^{2+}. J. Chem. Phys. **100**(9), 6422–6428 (1994)

47. Y.B. Kim, K. Stephan, E. Märk, T.D. Märk, Single and double ionization of nitric oxide by electron impact from threshold up to 180 eV. J. Chem. Phys. **74**(12), 6771–6776 (1981). https://doi.org/10.1063/1.441082

48. H.O. Folkerts, F.W. Bliek, M.C. de Jong, R. Hoekstra, R. Morgenstern, Dissociation of CO induced by He^{2+} ions: I. Fragmentation and kinetic energy release spectra. J. Phys. B Atomic Mol. Opt. Phys. **30**(24), 5833 (1997)

49. I. Ben-Itzhak, S.G. Ginther, K.D. Carnes, Multiple-electron removal and molecular fragmentation of co by fast F^{4+}, impact. Phys. Rev. A **47**, 2827–2837 (1993). https://doi.org/10.1103/PhysRevA.47.2827

50. K. Wohrer, G. Sampoll, R.L. Watson, M. Chabot, O. Heber, V. Horvat, Dissociation of multicharged co molecular ions produced in collisions with 97-MeV Ar^{14+}: dissociation fractions and branching ratios. Phys. Rev. A **46**, 3929–3934 (1992). https://doi.org/10.1103/PhysRevA.46.3929

51. I.H. Suzuki, N. Saito, Ionic fragmentation of NO following excitation of the NK-shell and the OK-shell electron. Laser Chem. **16**(1), 5–18 (1995)

52. G. Wei, Z. Jing-Yi, W. Bing-Xing, W. Yan-Qiu, W. Li, Fragmentation of CO in femtosecond laser fields. Chin. Phys. Lett. **26**(1), 013201 (2009). https://doi.org/10.1088/0256-307x/26/1/013201

53. T. Kaneyasu, K. Matsuda, M. Ehrich, M. Yoshino, K. Okuno, Fragmentation of N_2 and post collision effects in slow electron capture collisions of Kr^{8+} ion below 200 eV/amu. Phys. Scr. **T92**(1), 341–344 (2001). https://doi.org/10.1238/physica.topical.092a00341

54. K. Kayama, J.C. Baird, Spin-orbit effects and the fine structure in the $^3\Sigma_g^-$ ground state of O_2. J. Chem. Phys. **46**(7), 2604–2618 (1967). https://doi.org/10.1063/1.1841090

55. M. Lundqvist, D. Edvardsson, P. Baltzer, M. Larsson, B. Wannberg, Observation of predissociation and tunnelling processes in O_2^{2+}: a study using doppler free kinetic energy release spectroscopy and ab initio CI calculations. J. Phys. B Atomic Mol. Opt. Phys. **29**(3), 499–514 (1996)